Immunity
Article

RORγt+ Innate Lymphoid Cells Acquire a Proinflammatory Program upon Engagement of the Activating Receptor NKp44

Timor Glatzer,[1,12] Monica Killig,[1,12] Johannes Meisig,[3,7] Isabelle Ommert,[1] Merlin Luetke-Eversloh,[1] Marina Babic,[1,8] Daniela Paclik,[1] Nils Blüthgen,[3,7] Rainer Seidl,[9] Claudia Seifarth,[4] Jörn Gröne,[4] Minoo Lenarz,[5] Katharina Stölzel,[5] Dominik Fugmann,[6] Angel Porgador,[10] Anja Hauser,[2] Alexander Karlas,[11] and Chiara Romagnani[1,*]
[1]Innate Immunity
[2]Immunodynamics
Deutsches Rheuma-Forschungszentrum-Leibniz-Gemeinschaft, 10117 Berlin Germany
[3]Institute of Pathology
[4]Chirurgische Klinik und Hochschulambulanz I
[5]HNO-Klinik
[6]Klinik für Allgemein Visceral und Transplantationschirurgie
Charité–Universitätsmedizin, 12200 Berlin, Germany
[7]Institute for Theoretical Biology, Humboldt Universität, 10115 Berlin, Germany
[8]Department of Histology and Embryology, Faculty of Medicine, University of Rijeka, 51000 Rijeka, Croatia
[9]HNO-Klinik, Unfallkrankenhaus, 12683 Berlin, Germany
[10]The Shraga Segal Department of Microbiology and Immunology and the National Institute for Biotechnology in the Negev, Ben Gurion University of the Negev, 84105 Beer Sheva, Israel
[11]Molecular Biology Department, Max Planck Institute for Infection Biology, 10117 Berlin, Germany
[12]These authors contributed equally to this work
*Correspondence: romagnani@drfz.de
http://dx.doi.org/10.1016/j.immuni.2013.05.013

SUMMARY

RORγt+ innate lymphoid cells (ILCs) are crucial players of innate immune responses and represent a major source of interleukin-22 (IL-22), which has an important role in mucosal homeostasis. The signals required by RORγt+ ILCs to express IL-22 and other cytokines have been elucidated only partially. Here we showed that RORγt+ ILCs can directly sense the environment by the engagement of the activating receptor NKp44. NKp44 triggering in RORγt+ ILCs selectively activated a coordinated proinflammatory program, including tumor necrosis factor (TNF), whereas cytokine stimulation preferentially induced IL-22 expression. However, combined engagement of NKp44 and cytokine receptors resulted in a strong synergistic effect. These data support the concept that NKp44+ RORγt+ ILCs can be activated without cytokines and are able to switch between IL-22 or TNF production, depending on the triggering stimulus.

INTRODUCTION

Innate lymphoid cells (ILCs) comprise different lymphocyte populations sharing developmental requirements, such as dependence on the transcription factor inhibitor of DNA binding 2 (Id2) and γ-chain cytokines. In addition to conventional natural killer (cNK) cells and natural helper cells (ILC2), ILCs comprise a population of cells expressing CD127 (IL7Rα) and the orphan nuclear receptor RORγt, referred to as RORγt+ ILCs. RORγt+ ILCs include fetal lymphoid tissue-inducer (LTi) and adult LTi-like cells (Spits and Cupedo, 2012), which can be found after birth in secondary lymphoid organs or at mucosal sites (Cupedo et al., 2009; Mebius et al., 1997) and represent a major source of interleukin-22 (IL-22) (Cella et al., 2009; Cupedo et al., 2009; Luci et al., 2009; Sanos et al., 2009; Satoh-Takayama et al., 2008; Takatori et al., 2009). Expression of IL-22 by non-T cells is protective in inflammatory bowel disease (IBD) (Zenewicz et al., 2008), suggesting that IL-22 producing ILCs might modulate intestinal inflammation. IL-22 mediates these effects via its role in host defense against bacterial infection, mucosal wound healing, and intestinal epithelial cell homeostasis (Ouyang et al., 2011). Besides IL-22, RORγt+ ILCs produce several other cytokines including granulocyte macrophage colony-stimulating factor (GM-CSF), IL-13, IL-2, tumor necrosis factor (TNF), IL-17A and interferon-γ (IFN-γ) (Spits and Cupedo, 2012). Indeed, a potential pathogenic role of RORγt+ ILCs in experimental colitis models has also been shown in some reports (Buonocore et al., 2010; Geremia et al., 2011; Vonarbourg et al., 2010). The basis for the potential dual role of RORγt+ ILCs is poorly understood but certainly of major importance. RORγt+ ILCs might include distinct cell subsets characterized by different cytokine profiles and functional properties. In adult mice, two main subsets of RORγt+ ILCs are defined according to the expression of NKp46 (Luci et al., 2009; Sanos et al., 2009; Satoh-Takayama et al., 2008). In adult humans, RORγt+ ILCs can be dissected according to the expression of CD56 (Cupedo et al., 2009) or NKp44 (Cella et al., 2009). This heterogeneity might contribute to explain the distinct roles of RORγt+ ILCs in disease settings.

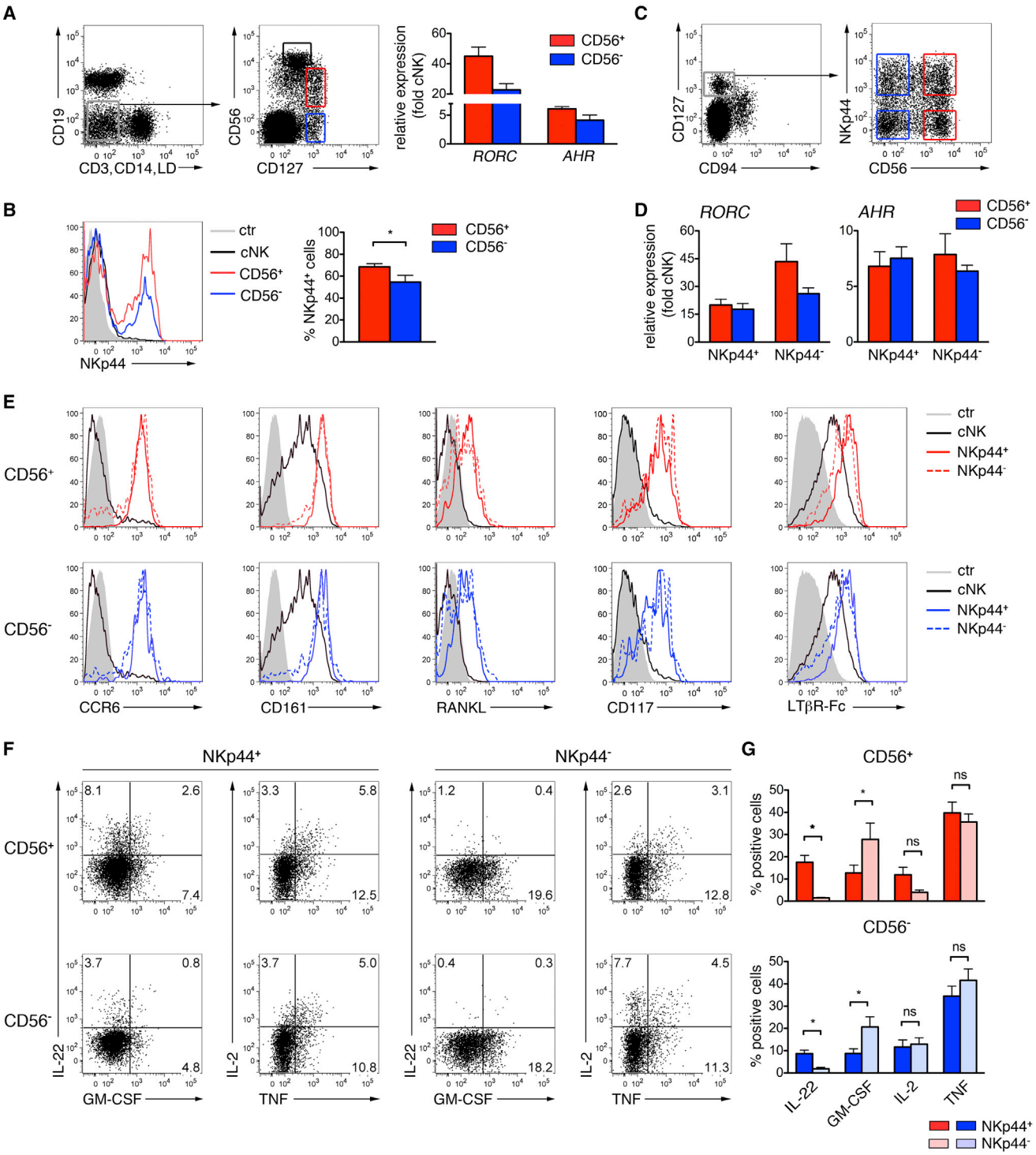

Figure 1. IL-22 but Not TNF Expression Is Confined to NKp44+ RORγt+ ILCs

Analysis of phenotype and cytokine profile of human tonsil-derived RORγt+ ILC subsets.

(A) Expression of CD127 and CD56 on viable (LD−) CD3− CD14− CD19− mononuclear cells (MNC) was analyzed by flow cytometry (FC) (left). *RORC* and *AHR* mRNA was detected by quantitative RT-PCR (qPCR) in FACS-sorted CD56+ CD127hi Lin− (CD3− CD14− CD19− CD94−) cells ("CD56+," red), CD56− CD127hi Lin− cells ("CD56−," blue) and CD56+ CD127lo/neg CD3− CD14− CD19− CD94+ cNK cells (right). Mean fold change ± SEM relative to cNK cells is plotted (n = 3), after normalizing to *GAPDH*.

(B) Expression of NKp44 was analyzed by FC after gating on CD56+ CD127hi Lin− (red line), CD56− CD127hi Lin− (blue line), cNK cells (black line), or CD56− CD127− Lin− cells (ctr, solid gray histograms), as control. One representative experiment (left) and mean percentage ± SEM (right) are shown (n = 6).

(C) Sorting strategy of CD127hi cells according to the expression of NKp44 and CD56, after gating on Lin− MNC.

(legend continued on next page)

Alternatively, it is possible that RORγt+ ILCs can acquire different effector functions depending on the activation context. IL-22 production by RORγt+ ILCs mainly depends on IL-23 and IL-1 released by antigen presenting cells (APCs) (Spits and Cupedo, 2012). However, RORγt+ ILCs might also directly sense the environment by the expression of aryl hydrocarbon receptor (AHR) (Kiss et al., 2011; Lee et al., 2012) or Toll-like receptor 2 (TLR2) (Crellin et al., 2010). Because TLR2 agonists induce IL-22 and/or IL-13 and IL-5 production only in the presence of IL-23 or IL-2 (Crellin et al., 2010), it still remains unclear whether RORγt+ ILCs can be activated completely independent of cytokines. Moreover, signals driving RORγt+ ILC expression of proinflammatory cytokines, such as TNF, need to be identified. In addition to cytokine receptors, innate cells employ RAG-independent strategies to sense pathogen-associated molecular patterns or danger signals induced in infected or transformed cells. For instance, cNK cells express several activating receptors (NKR), such as NKp46, NKp44, and NKp30. Although these three Ig-like receptors are all present in the human genome, only NKp46 displays high homology in mice. NKR engagement elicits cytokine release and degranulation of cytotoxic effector molecules in cNK cells. Although the nature of many NKR ligands remains elusive, their expression can be induced in infected or transformed cells (Moretta et al., 2001). Influenza virus (IV) hemagglutinin (HA) was shown to bind to NKp46 and NKp44; moreover, NKp46-deficient mice display increased susceptibility to lethal IV infection (Arnon et al., 2001; Gazit et al., 2006; Mandelboim et al., 2001). RORγt+ ILCs also express NKR. Although cross-linking of NKp46 or NK1.1 does not seem to elicit cytokine expression in RORγt+ ILCs derived from mouse small intestine (SI) (Satoh-Takayama et al., 2009), further analysis is required to clarify whether NKR engagement can trigger effector functions in different RORγt+ ILC subsets.

Here, we analyzed the signal requirements for cytokine expression in human RORγt+ ILCs and showed that engagement of the activating receptor NKp44 is sufficient to trigger selective TNF production and inflammatory gene signatures, while cytokine stimulation preferentially drives IL-22 expression in RORγt+ ILCs.

RESULTS

IL-22 but Not TNF Expression Is Confined to NKp44+ RORγt+ ILCs

Human RORγt+ ILCs can be identified as CD127hi Lin− cells (Cupedo et al., 2009) and dissected in different subsets according to the expression of CD56 and NKp44 (Cella et al., 2009; Cupedo et al., 2009). In order to assess the heterogeneity of tonsil RORγt+ ILCs, their ex vivo phenotype and functions were analyzed. Tonsil-derived CD56+ and CD56− RORγt+ ILCs displayed comparable expression of *RORC* and *AHR* (Figure 1A), as well as CD117, CCR6, CD161, lymphotoxin $\alpha_1\beta_2$ (as shown by staining with LTβR-Fc), and receptor activator of NF-κB ligand (RANKL) (see Figure S1A available online). Conversely, both RORγt+ ILC subsets neither expressed the ILC2 marker CRTH2 (Mjösberg et al., 2011), nor the cNK cell markers CD94 and T-box transcription factors T-bet and eomesodermin (Eomes) (Figure S1A). CD56+ and CD56− RORγt+ ILCs displayed also similar cytokine profiles, although percentage of producing cells was lower among CD56− RORγt+ ILCs (Figure S1B). IFN-γ, IL-17A, IL-13 (Figure S1B), and IL-5 (data not shown) were almost undetectable after intracellular staining, whereas both subsets produced IL-22, GM-CSF, IL-2, and TNF (Figure S1B). TNF protein could be detected not only intracellular, but also on the membrane (Figure S1C). Because expression of NKp44 was clearly bimodal with the CD56+ compartment being higher enriched in NKp44+ cells compared to the CD56− counterpart (Figure 1B), we investigated phenotype and cytokine profile of CD127hi Lin− ILC subsets sorted according to NKp44 and CD56 expression (Figure 1C). Although NKp44− and NKp44+ cells displayed comparable *RORC* and *AHR* transcripts (Figure 1D) and exhibited a similar surface phenotype (Figure 1E), IL-22 production was exclusively confined to the NKp44+ compartments, especially to the CD56+ NKp44+ one, whereas GM-CSF was significantly higher expressed among NKp44− cells. No differences in TNF production could be observed among the different subsets (Figures 1F and 1G). These data show that, although both NKp44− and NKp44+ CD127hi Lin− cells likely represent RORγt+ ILCs and display a comparable phenotype, expression of IL-22 is a specific hallmark of NKp44+ RORγt+ ILCs.

NKp44 Is Functional in RORγt+ ILCs and Its Engagement Induces Selective TNF Expression

RORγt+ ILCs were then analyzed for their expression and functionality of NK cell-activating receptors. In addition to NKp44, most RORγt+ ILCs expressed NKp30 and NKp46 (Figure 2A). Interestingly, only engagement of NKp44, but not of NKp30, NKp46, NKG2D (Figures 2B and 2C), CD161, or CD2 alone (Figure S2A) was able to elicit cytokine expression, namely TNF and few IL-2, in RORγt+ ILCs (Figures 2B–2D). The effects of combined engagement of NKp44 with NKp46 and NKp30 were similar to stimulation via NKp44 alone (Figure S2B). Conversely, almost no IL-22 or GM-CSF expression could be detected after NKp44 engagement (Figure 2D). Cytokine expression detected in RORγt+ ILCs by intracellular staining was also confirmed by measuring messenger RNA (mRNA) content and secreted protein at different time points after aNKp44 triggering (Figure S2C). Triggering of NKp44 resulted in cytokine expression only in NKp44+ but not in NKp44− RORγt+ ILCs (Figure 2E), whereas no major differences could be observed comparing CD56+ and CD56− RORγt+ ILCs (data not shown). Specificity of NKp44 engagement on RORγt+ ILCs was confirmed by the strong reduction of cytokine production in the presence of a different aNKp44 blocking monoclonal antibody (mAb), but not in the

(D) *RORC* and *AHR* mRNA in the four CD127hi Lin− subsets sorted as in (C) was measured and shown as described in (A) (n = 3).
(E) Expression of indicated markers analyzed by FC on the following populations: NKp44+ CD56+ CD127hi Lin− (red solid line), NKp44− CD56+ CD127hi Lin− (red dotted line), NKp44+ CD56− CD127hi Lin− (blue solid line), NKp44− CD56− CD127hi Lin− (blue dotted line), cNK cells (black solid line), or ctr cells (solid gray histograms). One representative experiment out of three is shown.
(F and G) CD127hi Lin− cells were FACS sorted as described in (C) and intracellular expression of the indicated cytokines was measured by FC after stimulation with PMA+Ionomycin (Iono)+IL-23. One representative experiment (F) and mean percentage ± SEM (G) are plotted (n = 6). See also Figure S1.

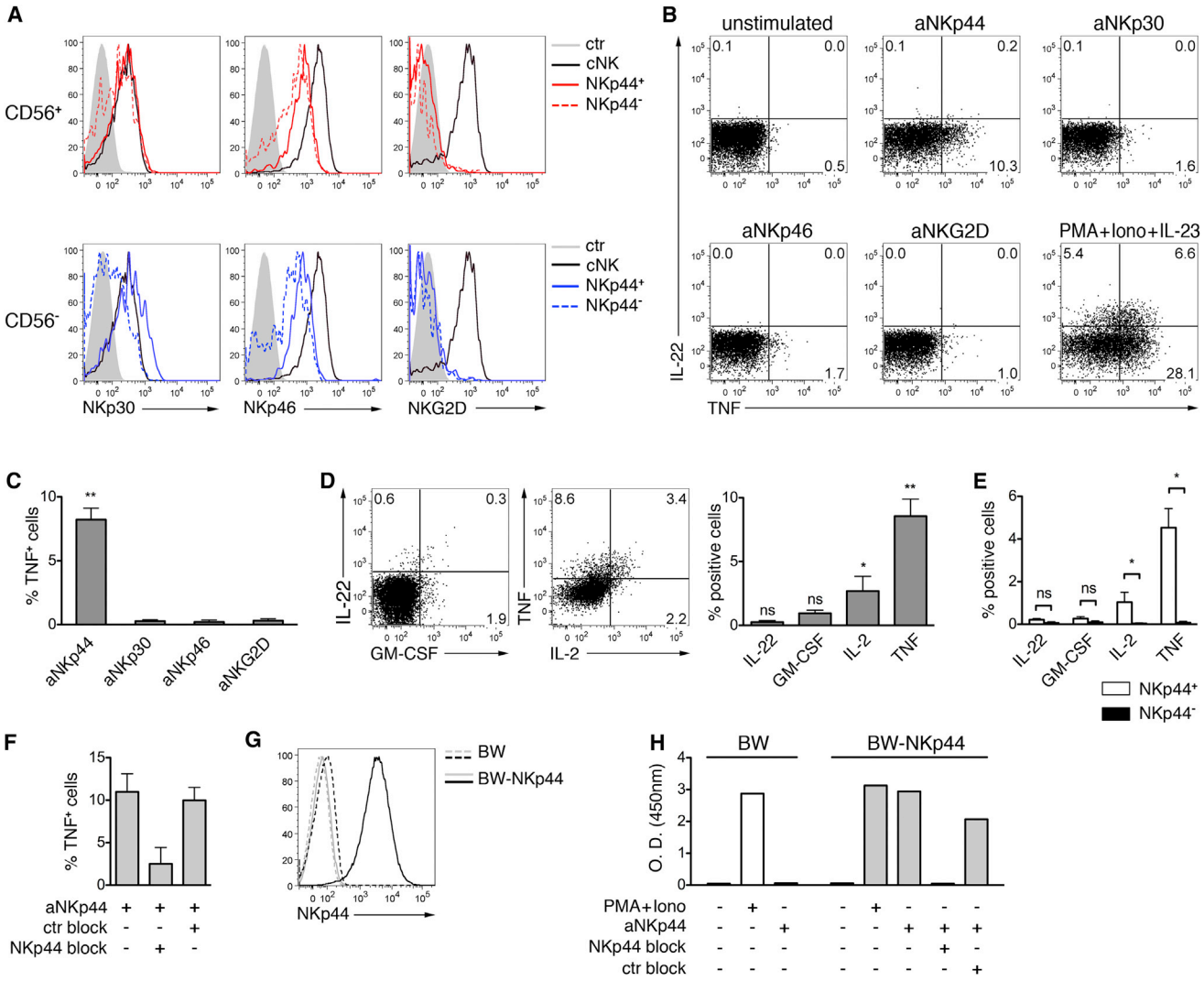

Figure 2. NKp44 Is Functional in RORγt+ ILCs and Its Engagement Induces Selective TNF Expression

Ex vivo analysis of cytokine profile of FACS-sorted RORγt+ ILCs derived from human tonsil after stimulation via different NKR.

(A) Surface expression of the indicated NKR was measured by FC after gating on different Lin− subsets, as described in Figure 1E. One representative experiment out of three is shown.

(B–D) Intracellular cytokine expression was analyzed by FC on FACS-sorted CD56+ CD127hi Lin− cells stimulated as indicated (B and C) or with cross-linking of NKp44 (aNKp44) only (D). One representative experiment (B and D, left) and mean percentage ± SEM (C and D, right) are shown (n = 6).

(E) FACS-sorted NKp44+ (white bars) and NKp44− (black bars) CD56+ CD127hi Lin− cells were stimulated with aNKp44, and mean percentage ± SEM of cytokine producing cells is shown (n = 6).

(F) FACS-sorted CD56+ CD127hi Lin− cells were stimulated with aNKp44 in the presence or absence of aNKp44-blocking (NKp44 block) or isotype control-blocking (ctr block) mAb. Intracellular expression of TNF was measured by FC, and mean percentage ± SEM of TNF+ cells is shown (n = 3).

(G) Expression of NKp44 was analyzed by FC on the murine thymoma BW reporter cells being either untransfected (BW, black dotted line) or transfected with NKp44–CD3ζ chimera (BW-NKp44, black solid line). Isotype controls are shown for BW cells (gray dotted line) and BW-NKp44 (gray solid line), respectively. One representative experiment out of three is shown.

(H) Stimulation of BW or BW-NKp44 reporter cells with the indicated stimuli. Expression of murine IL-2 by BW cells was measured by ELISA and plotted as mean absorbance (O.D. 450 nm) of duplicates from one representative experiment out of three. See also Figures S1 and S2.

presence of isotype control mAb (Figure 2F); moreover, aNKp44 selectively activated the mouse BW cell line transfected with a construct encoding human NKp44-CD3ζ-chain chimeric protein (BW-NKp44), thus displaying high surface expression of the NKp44 extracellular portion (Figure 2G), but not untransfected BW cells (Figure 2H). BW-NKp44 activation could be abolished by addition of aNKp44 blocking mAb (Figure 2H). These data show that engagement of NKp44 is sufficient to induce TNF, but not IL-22 expression, in RORγt+ ILCs.

Cytokines Preferentially Induce IL-22 Production in RORγt+ ILCs

Human RORγt+ ILCs can respond to several cytokines, such as IL-23, IL-1, IL-7, and IL-15, resulting in IL-22 production and/or

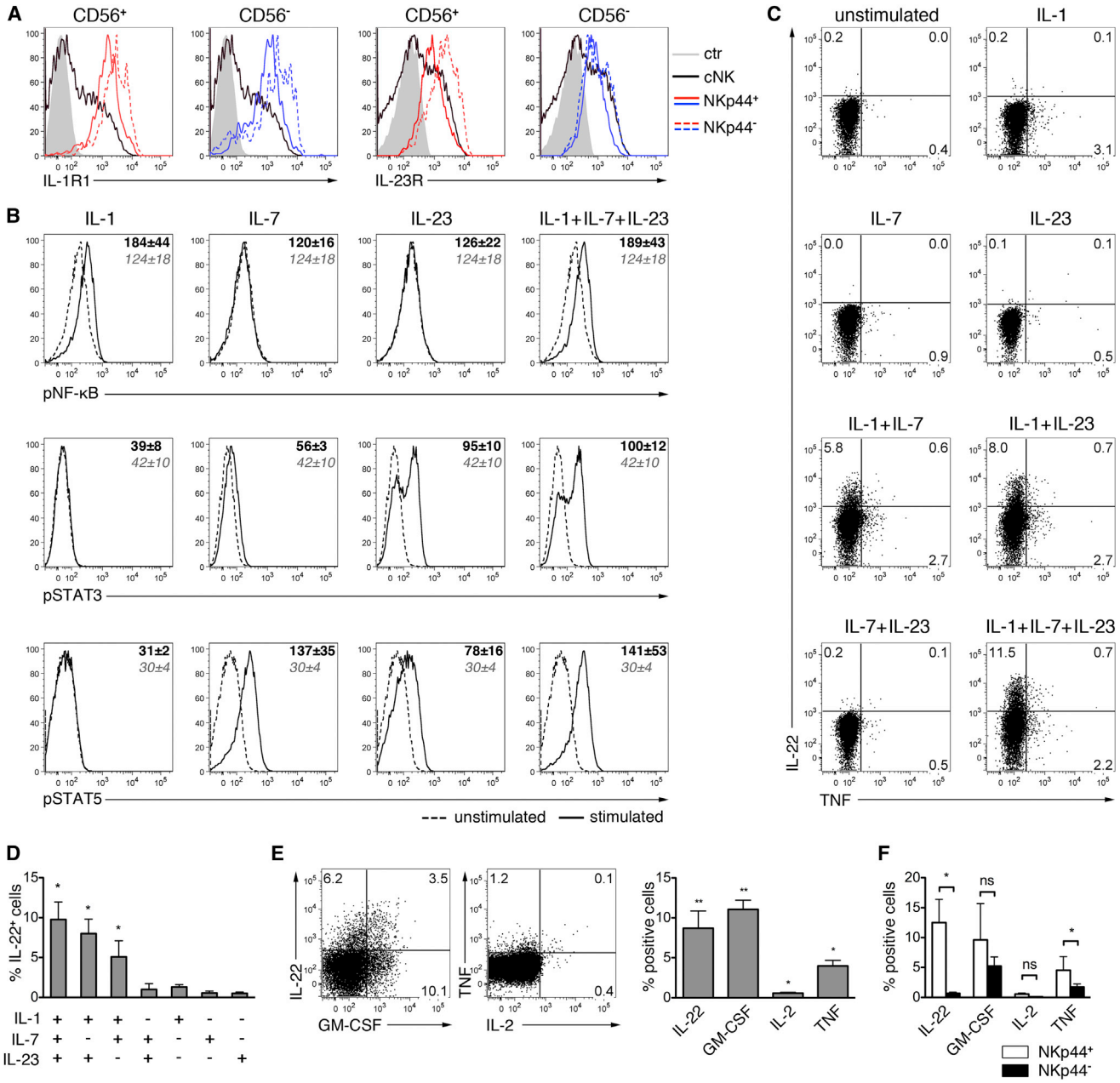

Figure 3. Cytokines Preferentially Induce IL-22 Production in RORγt+ ILCs

Ex vivo analysis of cytokine profile of FACS-sorted RORγt+ ILCs derived from human tonsil after stimulation with different cytokine combinations.

(A) Surface expression of IL-1R1 and IL-23R was measured by FC after gating as described in Figure 1E. One representative experiment out of three is shown.

(B) Intracellular expression of phosphorylated (p-) NF-κB, STAT3, and STAT5 was analyzed by FC in FACS-sorted CD56+ CD127hi Lin− cells either unstimulated (dotted line) or stimulated (solid line) for 15 min with the indicated cytokines. One representative experiment out of three is shown. Geometrical mean fluorescence intensity (MFI) ± SEM (n = 3) of unstimulated (italic numbers) or stimulated cells (bold numbers) is indicated in each plot.

(C–E) FACS-sorted CD56+ CD127hi Lin− cells were stimulated as indicated (C and D) or with IL-1+IL-7+IL-23 (E) and intracellular cytokine expression was measured by FC. One representative experiment (C) and (E, left) and mean percentage ± SEM of cytokine producing cells (D) and (E, right) are shown (n = 6).

(F) FACS-sorted NKp44+ (white bars) and NKp44− (black bars) CD56+ CD127hi Lin− cells were stimulated with IL-1+IL-7+IL-23 and cytokine expression was measured by FC. Mean percentage ± SEM of cytokine-producing cells is shown (n = 6). See also Figure S2.

proliferation (Cella et al., 2010; Crellin et al., 2010). Cytokine receptors for IL-7 (Figure 1A), IL-1, and IL-23 (Figure 3A) were highly expressed ex vivo on all RORγt+ ILC compartments and were functional because short stimulation with IL-1, IL-7, IL-23, or their combination promptly induced NF-κB, STAT5, and STAT3 phosphorylation, respectively (Figure 3B). Even though functional cytokine receptors were expressed, none of the above mentioned cytokines induced IL-22 expression in RORγt+ ILCs

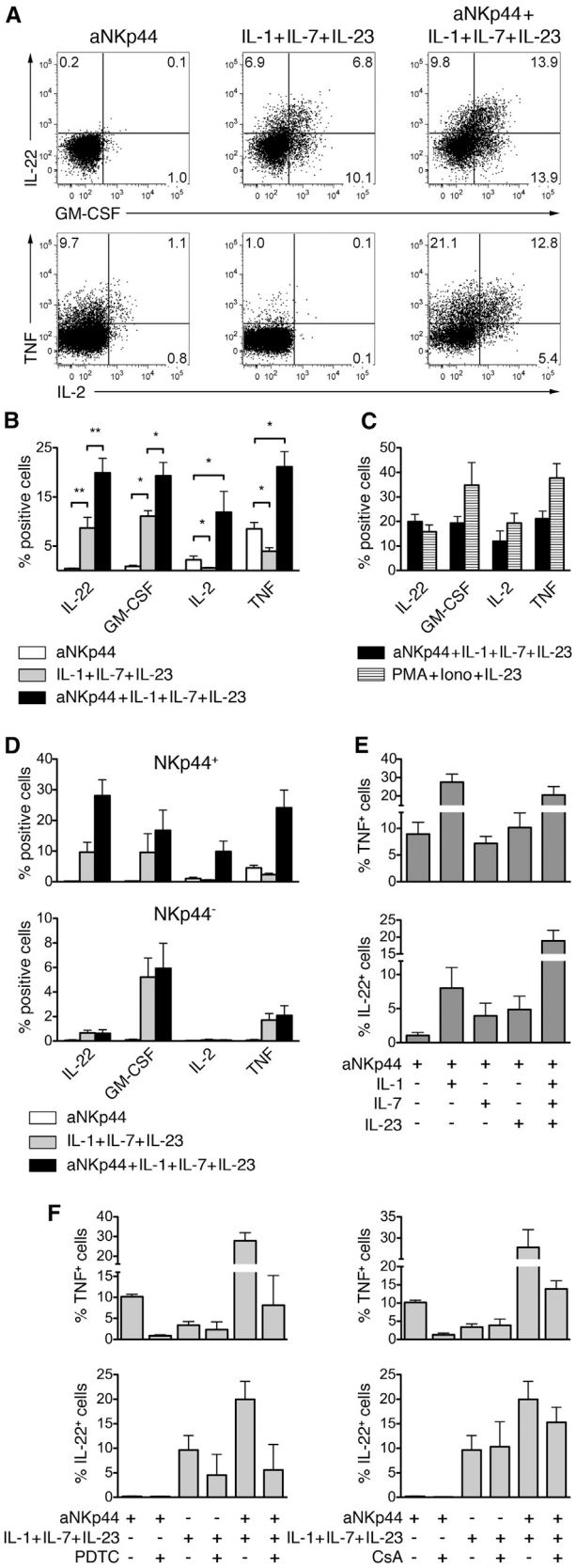

Figure 4. NKp44 Engagement Acts Synergistically with Cytokine Stimulation to Induce IL-22, GM-CSF, IL-2, and TNF

Ex vivo analysis of cytokine profile of human tonsil-derived FACS-sorted RORγt+ ILCs after stimulation with different combinations of aNKp44 and cytokines.

(A–C) Intracellular cytokine expression of FACS-sorted CD56+ CD127hi Lin− cells stimulated as indicated was measured by FC. One representative experiment (A) and mean percentage ± SEM (B and C) of cytokine producing cells are shown (n = 6).

(D) Intracellular cytokine expression of FACS-sorted NKp44+ (top) and NKp44− (bottom) CD56+ CD127hi Lin− cells stimulated as indicated is depicted as mean percentage ± SEM of cytokine-producing cells (n = 6).

(E and F) Intracellular cytokine expression of FACS-sorted CD56+ CD127hi Lin− cells stimulated as indicated in the presence or absence of 1 μM PDTC (F, left) or 100 nM CsA (F, right) is shown as mean percentage ± SEM (n ≥ 3). See also Figures S2 and S3.

when used alone. Only combination of IL-1 with IL-23, and to a less extent with IL-7, was able to induce IL-22 expression in RORγt+ ILCs. IL-1+IL-7+IL-23 stimulation resulted in the highest IL-22 production (Figures 3C and 3D). In addition to IL-22, IL-1+IL-7+IL-23 stimulation induced significant GM-CSF production, while only very low TNF and IL-2 could be observed (Figure 3E). Similar data could also be observed by measuring mRNA content and amounts of secreted cytokines at different time points (Figure S2C). IL-1+IL-7+IL-23 stimulation induced a similar cytokine profile in CD56+ and CD56− RORγt+ ILCs, despite the lower frequency of producers observed in the CD56− compartment (data not shown). Conversely, only NKp44+ cells produced IL-22 after IL-1+IL-7+IL-23 stimulation (Figure 3F), similar to what we observed after PMA+Iono+IL-23. Altogether, these data show that in contrast to NKp44 stimulation, triggering of cytokine receptors induces preferential expression of IL-22 but only very low TNF in RORγt+ ILCs.

Combined Engagement of NKp44 and Cytokine Receptors in RORγt+ ILCs Results in Strong Synergistic Effect

We next asked whether activating receptor and cytokine stimulation may act synergistically to induce cytokine expression in RORγt+ ILCs. Combination of NKp44 triggering with IL-1+IL-7+IL-23 stimulation resulted in enhanced expression of all cytokines analyzed (Figures 4A and 4B), at levels almost comparable to PMA+Iono+IL-23 stimulation (Figure 4C). As expected, this synergistic effect was confined to the NKp44+ cell compartment (Figure 4D). Strong synergy of NKp44 triggering with IL-1+IL-7+IL-23 stimulation could also be observed by measuring mRNA content and amounts of secreted IL-22, GM-CSF, IL-2, and TNF at different time points (Figure S2C). None of the stimuli analyzed was able to induce considerable expression of IL-17A (Figures S2D and S2E). Although IFN-γ, IL-13, or IL-5 could not be detected after any stimulation by intracellular staining (Figure S2D), induction of IFN-γ and IL-13 mRNA and minor amounts of secreted protein could be detected especially after aNKp44+IL-1+IL-7+IL-23 stimulation (Figure S2E). When we dissected the effects of each single cytokine (IL-1, IL-7, and IL-23) used in combination with NKp44 triggering, we observed that aNKp44 stimulation synergized with IL-23 or IL-7 to induce IL-22 expression but had only minor effects on TNF. Conversely, combination of IL-1 and aNKp44 increased both IL-22 and TNF expression (Figure 4E). Thus, NKp44 downstream signaling

enhanced IL-22 transcription in the presence of cytokines. In order to dissect the unique contribution of IL-1+IL-7+IL-23 and aNKp44 on cytokine production, we stimulated RORγt$^+$ ILCs in the presence of different inhibitors. Whereas Cyclosporin A (CsA), which preferentially blocks NFAT dephosphorylation, selectively decreased cytokine production after aNKp44, but not after IL-1+IL-7+IL-23 activation, the NF-κB inhibitor PDTC could efficiently inhibit both stimulations (Figure 4F). In agreement with previous data (Crellin et al., 2010), the pan Jak inhibitor I selectively decreased cytokine expression induced by IL-1+IL-7+IL-23, but not by aNKp44 stimulation (data not shown). Altogether, we showed that the signaling synergy achieved by IL-1+IL-7+IL-23 and NKp44 stimulation leads to optimal activation and cytokine production by RORγt$^+$ ILCs.

NK Cell Activating Receptors Are Functional in Mouse Splenic but Not in SI-Derived RORγt^{fm+} ILCs

Although NKp44 is not conserved between human and mouse (Moretta et al., 2001), a fraction of mouse RORγt$^+$ ILCs expresses other NKR, such as NK1.1 and NKp46 (Luci et al., 2009; Sanos et al., 2009; Satoh-Takayama et al., 2008). To test whether NKR were functional in mouse RORγt$^+$ ILCs, we took advantage of *Rorc*-Cre^{Tg}/*Rosa26R*-RFP fate-map (RORγt^{fm}) mice, in which all cells derived from RORγt$^+$ ILC precursors were marked by the RFP reporter. Thus, we analyzed whether triggering of NK1.1 or NKp46 could lead to cytokine expression in NKp46$^+$ RORγt^{fm+} Lin$^-$ cells, as compared to cNK cells (NKp46$^+$ RORγt^{fm-} Lin$^-$ cells). NK1.1 expression was high in spleen-derived, but lower or absent in SI-derived, RORγt^{fm+} ILCs (Figure S3A); moreover, IL-22 producing cells were enriched among SI-derived but not among splenic NKp46$^+$ RORγt^{fm+} ILCs (Figure S3B), in line with other reports (Vonarbourg et al., 2010). Engagement of NK1.1 alone, or together with IL-1+IL-23, induced IFN-γ and TNF production in mouse splenic NKp46$^+$ RORγt^{fm+} ILCs, similar to cNK cells, but not in NKp46$^+$ RORγt^{fm+} ILCs nor in cNK cells derived from SI (Figure S3B). NKp46 cross-linking induced some IFN-γ expression in splenic cNK cells, but not in NKp46$^+$ RORγt^{fm+} ILCs from any compartment (data not shown). These data support the concept that NKR are functional in mouse splenic, but not in SI-derived, NKp46$^+$ RORγt^{fm+} ILCs and that their engagement results in IFN-γ and TNF but not in IL-22 expression.

Engagement of NKp44 Ligands on Tumor Epithelial Cell Lines Leads to Cytokine Expression in RORγt$^+$ ILCs

NKp44 may recognize pathogen-derived molecules, including IV HA (Arnon et al., 2001), as well as undefined endogenous molecules upregulated in transformed cells (Byrd et al., 2007). Although H1N1 IV at different multiplicity of infection (MOI) did not induce significant cytokine expression in RORγt$^+$ ILCs (Figure S4A; data not shown), combination of IV with IL-1+IL-7+IL-23 resulted in higher cytokine expression compared to IL-1+IL-7+IL-23 alone (Figure S4A). However, IV-mediated activation of RORγt$^+$ ILCs did not appear to be NKp44-dependent because it could not be inhibited by addition of aNKp44-blocking mAb (Figure S4A). Therefore, we analyzed whether IV-infected cells could represent a better target for NKp44-recognition by RORγt$^+$ ILCs. By infecting Madin-Darby canine kidney (MDCK) cells, which are highly susceptible to IV infection, we observed that IV-infected or noninfected MDCK cells induced comparable cytokine expression in RORγt$^+$ ILCs (Figure S4B). Indeed, noninfected MDCK cells already displayed a high binding to human NKp44-Fc (Figures 5A and 5B) and were able to selectively activate BW-NKp44 reporter cells (Figure 5C). Stimulation of RORγt$^+$ ILCs with MDCK cells with or without IL-1+IL-7+IL-23 elicited cytokine expression similar to aNKp44 or aNKp44+IL-1+IL-7+IL-23, respectively, and could be completely abolished by aNKp44 blocking mAb (Figures 5D and 5E). Moreover, the human colorectal adenocarcinoma cell line SW620, which displayed NKp44-Fc binding (Figures 5A and 5B) and activated the BW-NKp44 reporter cell line, although to a much lower extent compared to MDCK cells (Figure 5C), was able to induce cytokine expression in RORγt$^+$ ILCs (Figures 5F and 5G) in a partially NKp44-dependent manner (Figure 5F). These data clearly indicate that RORγt$^+$ ILCs can be activated by the physiological interaction between NKp44 and its ligands expressed on transformed epithelial cells, recapitulating what we have observed by using aNKp44 or aNKp44+IL-1+IL-7+IL-23 stimulation.

NKp44 Triggering Induces Selective Regulation of Genes Related to Inflammatory Response

Selective engagement of NKp44 or cytokine receptors appeared to promote different functions in RORγt$^+$ ILCs. To confirm this hypothesis, we performed transcriptome analysis of highly purified CD56$^+$ CD127^{hi} ILCs ex vivo and after stimulation with aNKp44, IL-1+IL-7+IL-23, or aNKp44+IL-1+IL-7+IL-23. Compared to ex vivo, each stimulus induced significant regulation of a number of genes, of which a consistent fraction was coregulated under any of the tested conditions (Figure S5A), thus showing that exclusive engagement of NKp44 is an activating stimulus with a genome-wide regulating effect, similar to cytokine receptor stimulation. For instance, *IL2RA* (CD25) or *TNFRSF9* (CD137) transcripts were strongly upregulated after all stimulations (Figure S5B). In line with our functional data, each of the three stimulation conditions also resulted in a distinct expression pattern of a number of genes, referred to as "noncoregulated" (Figure S5A; Figure 6A). By hierarchical clustering of expression values of all noncoregulated genes, six main clusters were identified (Figures 6A and 6B). Gene ontology (GO) analysis was performed for each cluster with the aim to search for significant gene-sets enriched as compared to the entire genome (Figure 6A; Table S1). As shown in Figures 6A and 6B, Cluster 1 (green) and Cluster 5 (pink) included many genes downregulated by either aNKp44 and/or IL-1+IL-7+IL-23 stimulation. Among these clusters, genes related to negative regulation of biological processes or regulation of phosphate metabolic processes were overrepresented. Cluster 6 (yellow) included all noncoregulated genes with high fold changes. This cluster assembled two distinct set of genes, which were preferentially regulated either by aNKp44, such as *IL2*, *RCAN1*, *NR4A3* and *PTGS2* (Cox-2), or those whose expression was preferentially driven by cytokines, such as *IL22, SOCS2*, *SOCS3*, *SERPINA1*, *PRDM1* (Blimp-1), *IFNG*, and *GZMB* (granzyme B). Cluster 2 (blue) included genes that were significantly upregulated only by cytokines. In this cluster, we found an overrepresentation of genes related to apoptosis. Moreover, *IL26*, *STAT5A*, *CXCR5*, and *SERPINB1* could be identified as relevant cytokine-regulated

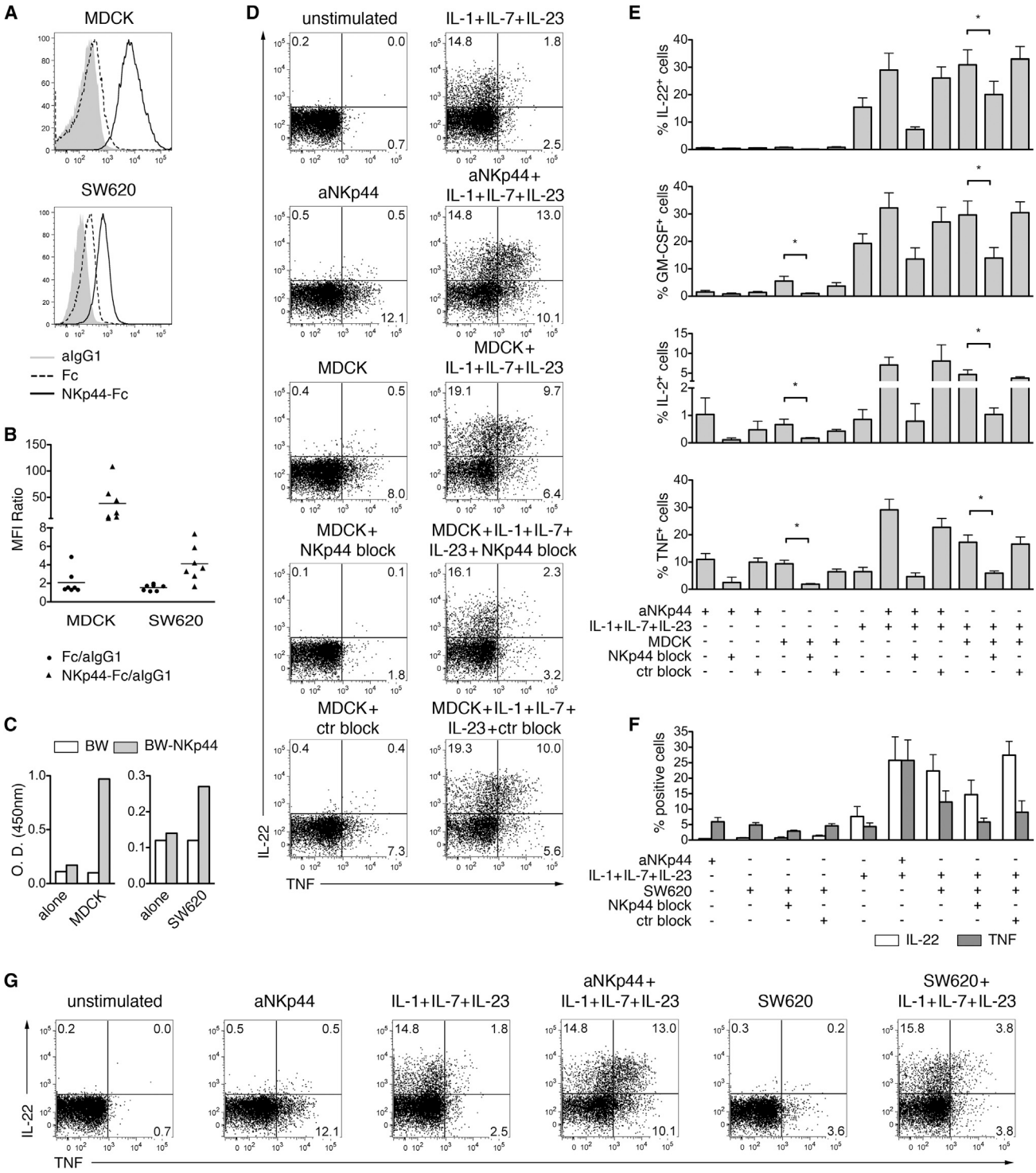

Figure 5. Engagement of NKp44 by Tumor Epithelial Cell Lines Results in Cytokine Expression in RORγt+ ILCs

Ex vivo analysis of cytokine profile of human tonsil-derived FACS-sorted RORγt+ ILCs after stimulation with NKp44 ligand-positive tumor epithelial cell lines. (A and B) Staining of MDCK and SW620 cell lines with NKp44-Fc (black solid line), Fc (black dotted line), or secondary anti-human IgG1 mAb (aIgG1) only (gray histogram) is shown as one representative histogram (A) or as MFI ratio of NKp44-Fc/aIgG1 (triangles) or of Fc/aIgG1 (circles) from six independent experiments (B). (C) BW or BW-NKp44 reporter cells were activated with irradiated MDCK (left) or SW620 (right) cells for 24 hr, and expression of murine IL-2 was measured by ELISA. Mean absorbance (O.D. 450 nm) of duplicates from one representative experiment out of three is shown.

(D–G) FACS-sorted CD56+ CD127hi Lin− cells were stimulated as indicated. Intracellular expression of the indicated cytokines was determined by FC, and one representative experiment (D and G) and mean ± SEM (n = 6) (E) (n ≥ 4) (F) are shown. See also Figure S4.

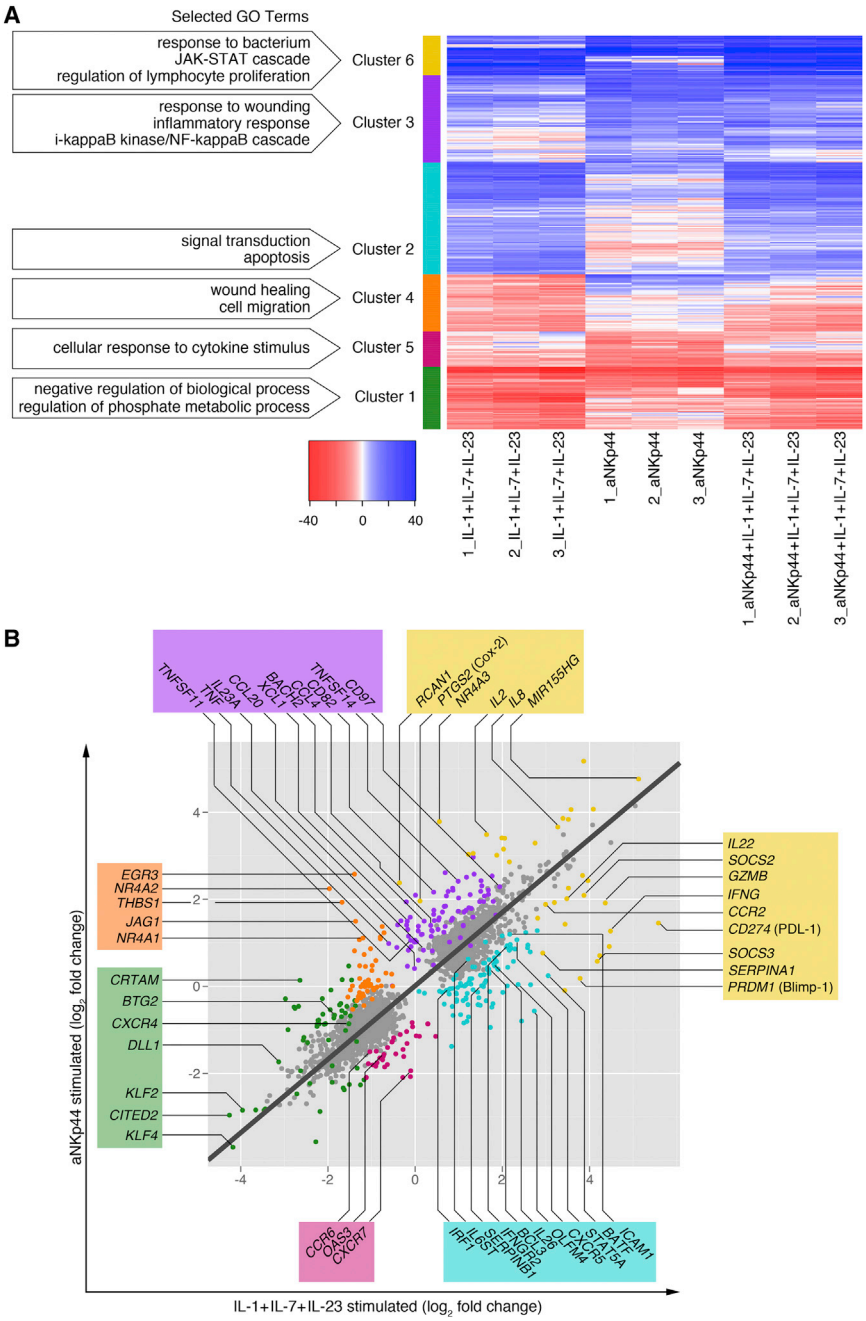

Figure 6. NKp44 Triggering Induces Selective Regulation of Genes Related to Inflammatory Response

Transcriptome analysis of human tonsil-derived FACS-sorted CD56^{+} CD127^{hi} Lin^{-} ILCs.

(A) Heatmap of differentially regulated genes in at least one of the three indicated stimuli compared to ex vivo. Plotted are z values of fold changes for three independent experiments. The color bar (left) indicates six clusters determined by hierarchical clustering (Ward's Method) on scaled expression values. Clusters were analyzed for GO enrichment and representative terms are depicted aside.

(B) Scatterplot of fold changes induced by stimulation with aNKp44 (y axis) and IL-1+IL-7+IL-23 (x axis) of all significantly regulated genes (in relation to ex vivo). Black line indicates direction of maximal variation of the fold change data, which was determined by principal component analysis. Gray dots represent genes showing largely correlated fold changes among the three stimulation conditions. Genes deviating from the axis of maximal variation are differentially regulated between the two stimulation conditions aNKp44 and IL-1+IL-7+IL-23. Colored dots represent all non-coregulated genes between all three stimulation conditions, as described in (A). Colors designate their cluster membership. Selected genes of each cluster have been labeled. See also Figure S5 and Table S1.

genes. Clusters 3 (violet) and 4 (orange) mostly included genes whose expression was preferentially driven by aNKp44 stimulation. These clusters were enriched in genes related to inflammatory response, response to wounding, I-κB/NF-κB cascade, and cell migration, thus suggesting that aNKp44 stimulation triggers a coordinated proinflammatory program. Among genes preferentially regulated by NKp44 engagement, we could identify *TNF*, *TNFSF11* (RANKL), *TNFSF14* (LIGHT), *CCL20*, *CCL4*, *XCL1*, *NR4A1*, *NR4A2*, or *THBS1* (thrombospondin). Most of the genes modulated by aNKp44+IL-1+IL-7+IL-23 stimulation were also found among the genes regulated by either aNKp44 or IL-1+IL-7+IL-23 stimulation (Figure S5C). Strong synergy occurred in selected gene transcription (e.g., *IL2*, *IL8*, *IL22*), when aNKp44+IL-1+IL-7+IL-23 stimulation was compared to aNKp44 or IL-1+IL-7+IL-23 alone (Figure S5C). Relevant gene signatures were confirmed by qPCR (Figure S5B). Some genes, such as *IL23A* (IL-23p19) were significantly regulated only by aNKp44+IL-1+IL-7+IL-23 stimulation, as measured by mRNA (Figure S5B), as well as by intracellular staining (Figure S5D). Conversely, IL-12/IL-23p40 protein (Figure S5D) and mRNA (data not shown) were undetectable. From this global analysis, it becomes evident that RORγt^{+} ILC stimulation via NKp44 elicits an overlapping and distinct gene signature compared to cytokines, especially by inducing genes related to inflammatory response, response to wounding, I-κB/NF-κB cascade, and cell migration.

Stimulus-dependent signatures induced in RORγt^{+} ILCs may impact the cross-talk with epithelial cells, which express the IL-22R. When activated with IL-1+IL-7+IL-23, but not with aNKp44 alone, RORγt^{+} ILCs induced in the intestinal epithelial cell (IEC) line HT-29 high mRNA expression of *IL10* and of regenerating islet-derived protein 3-alpha (*REG3A*), as well as β-defensin4 (*DEFB4A*). Expression of all three genes could be further enhanced in HT-29 by coculturing them together with RORγt^{+} ILCs activated with aNKp44+IL-1+IL-7+IL-23 (Figure S5E). Similar data were obtained when HT-29 were

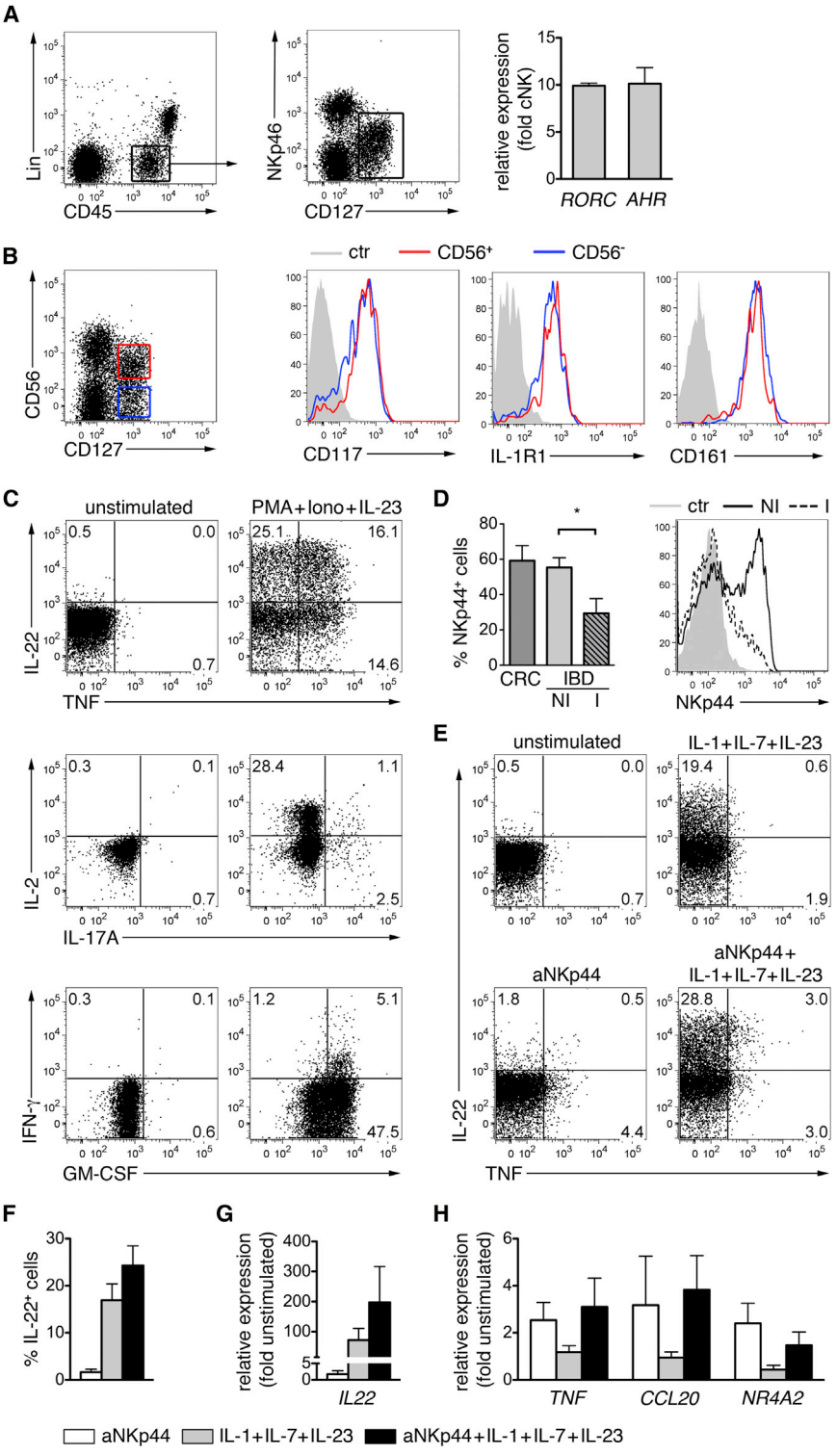

Figure 7. Characterization and NKp44 Responsiveness of Colon LP Derived RORγt+ ILCs

Phenotype and cytokine profile of RORγt+ ILCs derived from human colon LP isolated from CRC or IBD patients.

(A) Gating and sorting strategy to define CD127hi Lin− CD45+ cells in colon LP from CRC patients (left). *RORC* and *AHR* transcripts were determined by qPCR in FACS-sorted CD56+/− NKp46lo/neg CD127hi Lin− CD45+ cells (RORγt+ ILCs) and CD56+ NKp46hi CD127− CD3− CD14− CD19− CD45+ cells (cNK), as described in Figure 1A (n = 3).

(B) Expression of the indicated markers was analyzed by FC in MNC from colon LP of CRC patients after gating on CD56+ (red line) and CD56− (blue line) CD127hi Lin− CD45+ ILCs. One representative experiment out of six is shown.

(C) FACS-sorted CD127hi Lin− CD45+ ILCs derived from colon LP of CRC patients were stimulated for 6 hr with PMA+Iono+IL-23. Intracellular cytokine expression detected by FC is shown as one representative experiment (n = 3).

(D) NKp44 expression on MNC from macroscopically noninflamed (NI) or inflamed (I) colon LP samples from the same IBD patient or from nonaffected colon LP isolated from CRC patients was determined by FC, after gating on CD56+ CD127hi Lin− CD45+. Mean percentage ± SEM of NKp44+ cells (CRC n = 4; IBD n = 6) (left) and one representative experiment (right) are shown.

(E and F) FACS-sorted CD127hi Lin− CD45+ cells derived from colon LP of CRC patients were stimulated with the specified stimuli and intracellular expression of the indicated cytokines was measured by FC. One representative experiment (E) and mean percentage ± SEM of IL-22+ cells (F) are shown (n = 3).

(G and H) mRNA transcripts of the specified genes were analyzed by qPCR after stimulation of FACS-sorted CD127hi Lin− CD45+ cells derived from colon LP of CRC patients. Data were normalized to *GAPDH* and shown as mean fold change ± SEM relative to unstimulated cells (n = 3).

incubated with supernatants derived from RORγt+ ILCs activated via the same stimuli (data not shown). These data support the concept that RORγt+ ILCs might exert different effects on IECs depending on the present stimulus and that RORγt+ ILC activation with aNKp44+IL-1+IL-7+IL-23 promotes a strong response in IECs.

Characterization and NKp44 Responsiveness of Colon-Derived RORγt+ ILCs

RORγt+ ILCs have been described in human gut lamina propria (LP) (Cella et al., 2009; Geremia et al., 2011; Takayama et al., 2010). Indeed, a consistent population of CD127hi Lin− CD45+ cells could be isolated from macroscopically inflamed or noninflamed colon mucosa derived from IBD patients, as well as from nonaffected colon of patients undergoing colectomy for colorectal cancer (CRC) (Figure 7A). Similar to tonsil-derived RORγt+ ILCs, colon LP CD127hi Lin− CD45+ cells displayed low expression of NKp46 and were enriched in *RORC* and *AHR* transcripts (Figure 7A). No difference in CD117, IL-1R1, or CD161 expression could be detected among colon LP RORγt+ ILCs dissected according to CD56

(Figure 7B). PMA+Iono+IL-23 stimulation resulted in numerous cells producing IL-22, GM-CSF, IL-2, and TNF, whereas only a few cells expressed IFN-γ or IL-17A (Figure 7C). NKp44 was present on the surface of a consistent fraction of colon LP RORγt+ ILCs, and its expression was comparable between noninflamed colon of IBD patients and nonaffected colon of CRC control patients. Notably, NKp44 expression among RORγt+ ILCs was significantly lower in inflamed compared to noninflamed colon LP samples from the same IBD patients (Figure 7D). Stimulation of colon LP RORγt+ ILCs with IL-1+IL-7+IL-23 led to strong induction of IL-22 but only to low TNF expression. NKp44 engagement could clearly synergize with cytokine stimulation to enhance IL-22 expression (Figures 7E–7G), although only very few cells were positive for intracellular TNF (Figure 7E). In order to confirm the efficacy of NKp44 triggering in colon LP RORγt+ ILCs, mRNA expression of *TNF* as well as *CCL20* and *NR4A2*, which were all regulated by NKp44 engagement in tonsil RORγt+ ILCs (Figures 6B; Figure S5B), were analyzed. In line with our tonsil data, mRNA of all three genes was selectively induced after NKp44 triggering, thus further corroborating its functionality in colon LP RORγt+ ILCs (Figure 7H). Altogether, these data show that colon LP RORγt+ ILCs represent a population strongly enriched in RORγt+ NKp44+ IL-22-producing cells, which is responsive to both IL-1+IL-7+IL-23 and NKp44 stimulation, similar to their tonsil counterpart.

DISCUSSION

The mechanisms underlying the nature of the dual role of RORγt+ ILCs in regulation of inflammatory diseases are still poorly understood. RORγt+ ILCs might include distinct cell subsets characterized by different cytokine production and functional properties. Our analysis of human tonsil CD127hi ILC subsets dissected according to both CD56 and NKp44 revealed that, although all subsets analyzed could be collectively referred to as RORγt+ ILCs, expression of IL-22 was strictly confined to the NKp44+ fraction, in line with a recent report (Hoorweg et al., 2012). Conversely, expression of TNF was not confined to a particular subset but rather represented a common feature of all RORγt+ ILC subsets.

One alternative explanation for the double nature of RORγt+ ILCs could be that these cells display distinct effector functions depending on their context of activation; for instance, after engagement of cytokine receptors or of innate sensors. This concept is supported by previous evidence showing that activation of RORγt+ ILCs with TLR2 agonists together with IL-23 induces IL-22 production, whereas combination of TLR2 agonists with IL-2 results in IL-22 and in IL-13 and IL-5 expression (Crellin et al., 2010). In line with this idea, we show that cytokine or aNKp44 stimulation could trigger partially distinct signatures in RORγt+ ILCs. Importantly, activation via cytokine receptors induced a preferential upregulation of IL-22, which mainly drives tissue repair and mucosal homeostasis (Ouyang et al., 2011), but resulted in only low TNF expression. Besides IL-22, cytokine stimulation of RORγt+ ILCs upregulated the expression of alpha-1 antitrypsin (*SERPINA1*) and leukocyte elastase inhibitor (*SERPINB1*), which are involved in tissue protection and are also induced in IECs by IL-22 stimulation (Cella et al., 2009). Conversely, NKp44 triggering induced TNF expression in the frame of a coordinated proinflammatory program. Thus, our data imply that NKp44+ RORγt+ ILCs can switch between IL-22 and TNF production depending on the triggering stimulus. Little evidence has been provided that RORγt+ ILCs can sense and react to the environment directly, independent of proinflammatory cytokines. In humans, it was shown that RORγt+ ILCs could be activated by TLR2 in combination with IL-23 or IL-2 (Crellin et al., 2010). Our observation that NKp44 triggering alone elicited TNF production in RORγt+ ILCs strongly supports the idea that RORγt+ ILCs are endowed with pattern recognition receptors directly sensing the environment, regardless of cytokine stimulation. Although HA of H1N1 IV has been previously identified as a potential ligand of NKp44 (Arnon et al., 2001), IV infection of RORγt+ ILCs did not lead to consistent cytokine expression, in contrast to what has been shown for cNK cells (Jost et al., 2011). Moreover, cytokine expression induced after RORγt+ ILC stimulation with IV+IL-1+IL-7+IL-23 did not appear to be NKp44-dependent. Because a critical point for the NKp44 (or NKp46) interaction with HA is the glycosylation of the receptor, we cannot exclude that NKp44 might be differently glycosylated in RORγt+ ILCs and NK cells. Further investigation should validate this hypothesis. However, we could clearly show that engagement of undefined NKp44 ligands on transformed epithelial cell lines induced NKp44-dependent cytokine expression in RORγt+ ILCs. Our data suggest that high-affinity conserved NKp44-ligands, able to activate RORγt+ ILCs, might be also expressed on the canine MDCK cell line. Because NKp44 is also expressed in canine NK cells (Huang et al., 2008), NKp44 ligands might have coevolved together with their receptor as shown for B7H6 and NKp30 (Flajnik et al., 2012). Nonetheless, the nature of the NKp44 ligands eliciting inflammatory signatures in RORγt+ ILCs remains to be explored, and only their identification will comprehensively enlighten the physiological relevance of NKp44 engagement in RORγt+ ILCs. Until then, we can only speculate that NKp44 recognition of ligands expressed by microorganisms or IECs could participate in fighting selected pathogens, restraining gut microflora, or even regulating IEC homeostasis at steady state or during inflammation. Because TNF represents a major proinflammatory cytokine involved in the pathogenesis of several chronic autoimmune diseases, the in vivo role of RORγt+ ILC-derived TNF certainly deserves further investigation. Besides TNF, other proinflammatory cytokines such as IFN-γ or IL-17A are shown to be produced by RORγt+ ILCs (Cella et al., 2010; Geremia et al., 2011). Although only low expression of IFN-γ protein could be detected, *IFNG* transcripts were induced after IL-1+IL-7+IL-23 stimulation, suggesting that IFN-γ might undergo posttranscriptional regulation in stimulated RORγt+ ILCs. A discrepancy between protein and mRNA content for GM-CSF and TNF could also be observed. Interestingly, MAP-kinase-activated protein kinase (MK2), which modulates the translation and stability of TNF mRNA (Kotlyarov et al., 1999), was upregulated in stimulated tonsil RORγt+ ILCs (data not shown), thus likely contributing to modulate TNF expression in RORγt+ ILCs.

Finally, in line with previous data (Luci et al., 2009; Satoh-Takayama et al., 2009), we have shown that NKR triggering did not induce cytokine expression in mouse SI-derived NKp46+ RORγtfm+ ILCs. Conversely, mouse splenic NKp46+ RORγtfm+ ILCs produced IFN-γ and TNF in response to NK1.1 stimulation,

suggesting that the ability of RORγt$^+$ ILCs to produce proinflammatory cytokines after NKR engagement is partially conserved. However, because mouse splenic NKp46$^+$ RORγt^{fm+} ILCs are not proficient IL-22 producers, mouse NKR might not play any role in IL-22 induction.

Altogether, our data clearly demonstrate that RORγt$^+$ ILCs can directly sense the environment by engagement of NKp44 and that selective triggering of activating or cytokine receptors contributes to determine the cytokine profile and functional properties of NKp44$^+$ RORγt$^+$ ILCs. Hence, NKp44 might represent an interesting therapeutic target to modulate proinflammatory versus protective features of RORγt$^+$ ILCs during inflammatory diseases.

EXPERIMENTAL PROCEDURES

Cell Isolation and Flow Cytometry

Cell populations from human tonsils were isolated from patients undergoing tonsillectomy, as previously described (Ryon, 2001). Gut LP cells were isolated from CRC or IBD patients undergoing colectomy, by using a modified version of the protocol of Bull and Bookman (Bull and Bookman, 1977). Written informed consent was obtained from all patients prior to sample acquisition and experiments have been approved by the Ethics Committee of the Charité Medical University, Berlin (EA4/106/11 and EA1/107/10). RORγt$^+$ ILCs were enriched by using magnetic cell sorting (MACS): CD3$^+$ T cells were first depleted by using anti-CD3 microbeads and CD127$^+$ cells were then positively selected by using CD127 microbead kit. Alternatively, CD56$^+$ RORγt$^+$ ILCs were directly enriched by using anti-CD56 microbeads (all Miltenyi Biotec). All MACS enriched cell fractions were subsequently FACS sorted to high purity (above 95%) by using FACSAria II cell sorter (BD Biosciences), according to markers indicated in the figure legends. Flow cytometric analysis was performed by using BD FACSCanto II or Fortessa employing FACSDiva Software (BD Biosciences), and data were analyzed by using FlowJo software (Tree Star). Further details and list of antibodies used have been included in Supplemental Information. Isolation of murine cells is described in the Supplemental Information. Experiments were approved and in accordance with local animal care and use committees.

In Vitro Stimulation, Intracellular Staining, and ELISA/CBA

We cultured 20,000 cells of FACS-sorted human ILC subsets in RPMI containing 10% human AB serum (Lonza), 100 U/mL Penicillin, and 0.1 mg/ml Streptomycin (PAA Laboratories). When indicated, PMA (20 ng/ml), Ionomycin (1 μg/ml; both Sigma), IL-1, IL-7 (Miltenyi Biotec), and IL-23 (R&D Systems; 50 ng/ml each) were added. For activating receptor stimulation, 20 μg/ml of biotinylated antibodies specific for NKp44 (2.29), NKp30 (AF29-4D12), NKp46 (9E2), CD2 (LT2), CD161 (191B8), or NKG2D (BAT221) were conjugated to anti-biotin MACSiBead particles (all Miltenyi Biotec) and used to stimulate human RORγt$^+$ ILCs at bead:cell ratio of 5:1. When indicated, cells were incubated with 1 μM PDTC (Calbiochem), 100 nM CsA (Sigma), or 1 μM of Jak inhibitor I (Millipore) at 37°C for 1 hr prior to stimulation. For blockade of NKp44 engagement, cells were incubated with anti-NKp44 (KS38, IgM) or anti-CD56 (A6-220, IgM isotype control) mAb (10 μg/ml) at 4°C for 1 hr prior to stimulation. KS38 and A6-220 were kindly provided by S. Parolini, University of Brescia, and A. Moretta, University of Genova, Italy, respectively.

Intracellular cytokine staining was performed either after 20 hr (human tonsil), if not indicated differently, or 6 hr (human gut) of stimulation in the presence of Brefeldin A (10 μg/ml) (Sigma). Cells were fixed with 2% paraformaldehyde (Electron Microscopy Services) and stained intracellular in the presence of 0.5% saponin (Sigma) in PBS. Activated NF-κB, STAT5, and STAT3 were detected after 15 min stimulation by using Cytofix buffer and PermIII (all BD Biosciences). Cytokines in cell culture supernatants of stimulated RORγt$^+$ ILCs were determined by using Cytometric Bead Array (BD Biosciences) with the exception of IL-22, which was detected by ELISA (Biolegend), according to manufacturer's instruction. Further details have been included in Supplemental Information. Reagents and experimental procedures employing murine cells are described in the Supplemental Information.

Activation of NKp44–CD3ζ Chimera (BW-NKp44)

Murine BW thymoma cells untransfected and BW-NKp44 stable transfectants were a kind gift of O. Mandelboim (Hebrew University Hadassah Medical School, Jerusalem, Israel). The experimental procedure is described in Supplemental Information.

Quantitative RT-PCR (qPCR)

mRNA was isolated from cells by using NucleoSpin RNAII (Macherey Nagel). cDNA was synthesized by using Reverse Transcription Reagents and assayed by qPCR in duplicates by using a StepOne Plus real-time PCR system and TaqMan Gene expression assays (all Applied Biosystems). A list of all TaqMan Gene expression assays employed is included in Supplemental Information. mRNA content was normalized to *GAPDH* expression. Mean relative gene expression was determined by using the ΔΔCT method.

Microarray Gene Expression Profiling

RORγt$^+$ ILCs were stimulated for 3.5 hr and RNA was isolated by using NucleoSpin RNAII. cDNA was synthesized from 100 ng total RNA (Ambion) pooled from four or two donors. cRNA was synthesized using Enzo RNA Transcript Labeling kit (Affymetrix). Three replicates of biotinylated cRNA (15 μg) per group were fragmented and hybridized to 12 Affymetrix HG U133 plus 2.0 GeneChips by using standard Affymetrix protocols. The arrays were scanned with an Affymetrix GeneChip Scanner 3000. Further details have been included in Supplemental Information.

Statistical Analysis

Wilcoxon signed rank two-tailed test was employed for statistical analysis of data sets consisting of at least six independent experiments (*$p < 0.05$, **$p < 0.01$, ***$p < 0.001$) by using GraphPad Prism (GraphPad Software).

ACCESSION NUMBERS

Raw data of resulting chips were uploaded to Gene Expression Omnibus (GEO) database repository under the following series accession number: GSE43409.

SUPPLEMENTAL INFORMATION

Supplemental Information includes five figures, one table, and Supplemental Experimental Procedures and can be found with this article online at http://dx.doi.org/10.1016/j.immuni.2013.05.013.

ACKNOWLEDGMENTS

We thank Toralf Kaiser and Jenny Kirsch for cell sorting, Andreas Grützkau for discussion about the microarrays, Heidi Schliemann for excellent technical assistance, Andrey Kruglov and Ofer Mandelboim for sharing reagents and helpful discussion, and Simon Fillatreau and Jens Geginat for critical reading of the manuscript and discussion. This work was supported by the Deutsche Forschungsgemeinschaft (DFG) SFB 633 and SFB 650 (to C.R.).

Received: May 31, 2012
Accepted: March 5, 2013
Published: June 20, 2013

REFERENCES

Arnon, T.I., Lev, M., Katz, G., Chernobrov, Y., Porgador, A., and Mandelboim, O. (2001). Recognition of viral hemagglutinins by NKp44 but not by NKp30. Eur. J. Immunol. *31*, 2680–2689.

Bull, D.M., and Bookman, M.A. (1977). Isolation and functional characterization of human intestinal mucosal lymphoid cells. J. Clin. Invest. *59*, 966–974.

Buonocore, S., Ahern, P.P., Uhlig, H.H., Ivanov, I.I., Littman, D.R., Maloy, K.J., and Powrie, F. (2010). Innate lymphoid cells drive interleukin-23-dependent innate intestinal pathology. Nature *464*, 1371–1375.

Byrd, A., Hoffmann, S.C., Jarahian, M., Momburg, F., and Watzl, C. (2007). Expression analysis of the ligands for the Natural Killer cell receptors NKp30 and NKp44. PLoS ONE *2*, e1339.

Cella, M., Fuchs, A., Vermi, W., Facchetti, F., Otero, K., Lennerz, J.K., Doherty, J.M., Mills, J.C., and Colonna, M. (2009). A human natural killer cell subset provides an innate source of IL-22 for mucosal immunity. Nature *457*, 722–725.

Cella, M., Otero, K., and Colonna, M. (2010). Expansion of human NK-22 cells with IL-7, IL-2, and IL-1beta reveals intrinsic functional plasticity. Proc. Natl. Acad. Sci. USA *107*, 10961–10966.

Crellin, N.K., Trifari, S., Kaplan, C.D., Satoh-Takayama, N., Di Santo, J.P., and Spits, H. (2010). Regulation of cytokine secretion in human CD127(+) LTi-like innate lymphoid cells by Toll-like receptor 2. Immunity *33*, 752–764.

Cupedo, T., Crellin, N.K., Papazian, N., Rombouts, E.J., Weijer, K., Grogan, J.L., Fibbe, W.E., Cornelissen, J.J., and Spits, H. (2009). Human fetal lymphoid tissue-inducer cells are interleukin 17-producing precursors to RORC+ CD127+ natural killer-like cells. Nat. Immunol. *10*, 66–74.

Flajnik, M.F., Tlapakova, T., Criscitiello, M.F., Krylov, V., and Ohta, Y. (2012). Evolution of the B7 family: co-evolution of B7H6 and NKp30, identification of a new B7 family member, B7H7, and of B7's historical relationship with the MHC. Immunogenetics *64*, 571–590.

Gazit, R., Gruda, R., Elboim, M., Arnon, T.I., Katz, G., Achdout, H., Hanna, J., Qimron, U., Landau, G., Greenbaum, E., et al. (2006). Lethal influenza infection in the absence of the natural killer cell receptor gene Ncr1. Nat. Immunol. *7*, 517–523.

Geremia, A., Arancibia-Cárcamo, C.V., Fleming, M.P., Rust, N., Singh, B., Mortensen, N.J., Travis, S.P., and Powrie, F. (2011). IL-23-responsive innate lymphoid cells are increased in inflammatory bowel disease. J. Exp. Med. *208*, 1127–1133.

Hoorweg, K., Peters, C.P., Cornelissen, F., Aparicio-Domingo, P., Papazian, N., Kazemier, G., Mjosberg, J.M., Spits, H., and Cupedo, T. (2012). Functional Differences between Human NKp44(-) and NKp44(+) RORC(+) Innate Lymphoid Cells. Frontiers in Immunology *3*, 72.

Huang, Y.C., Hung, S.W., Jan, T.R., Liao, K.W., Cheng, C.H., Wang, Y.S., and Chu, R.M. (2008). CD5-low expression lymphocytes in canine peripheral blood show characteristics of natural killer cells. J. Leukoc. Biol. *84*, 1501–1510.

Jost, S., Reardon, J., Peterson, E., Poole, D., Bosch, R., Alter, G., and Altfeld, M. (2011). Expansion of 2B4+ natural killer (NK) cells and decrease in NKp46+ NK cells in response to influenza. Immunology *132*, 516–526.

Kiss, E.A., Vonarbourg, C., Kopfmann, S., Hobeika, E., Finke, D., Esser, C., and Diefenbach, A. (2011). Natural aryl hydrocarbon receptor ligands control organogenesis of intestinal lymphoid follicles. Science *334*, 1561–1565.

Kotlyarov, A., Neininger, A., Schubert, C., Eckert, R., Birchmeier, C., Volk, H.D., and Gaestel, M. (1999). MAPKAP kinase 2 is essential for LPS-induced TNF-alpha biosynthesis. Nat. Cell Biol. *1*, 94–97.

Lee, J.S., Cella, M., McDonald, K.G., Garlanda, C., Kennedy, G.D., Nukaya, M., Mantovani, A., Kopan, R., Bradfield, C.A., Newberry, R.D., and Colonna, M. (2012). AHR drives the development of gut ILC22 cells and postnatal lymphoid tissues via pathways dependent on and independent of Notch. Nat. Immunol. *13*, 144–151.

Luci, C., Reynders, A., Ivanov, I.I., Cognet, C., Chiche, L., Chasson, L., Hardwigsen, J., Anguiano, E., Banchereau, J., Chaussabel, D., et al. (2009). Influence of the transcription factor RORgammat on the development of NKp46+ cell populations in gut and skin. Nat. Immunol. *10*, 75–82.

Mandelboim, O., Lieberman, N., Lev, M., Paul, L., Arnon, T.I., Bushkin, Y., Davis, D.M., Strominger, J.L., Yewdell, J.W., and Porgador, A. (2001). Recognition of haemagglutinins on virus-infected cells by NKp46 activates lysis by human NK cells. Nature *409*, 1055–1060.

Mebius, R.E., Rennert, P., and Weissman, I.L. (1997). Developing lymph nodes collect CD4+CD3- LTbeta+ cells that can differentiate to APC, NK cells, and follicular cells but not T or B cells. Immunity *7*, 493–504.

Mjösberg, J.M., Trifari, S., Crellin, N.K., Peters, C.P., van Drunen, C.M., Piet, B., Fokkens, W.J., Cupedo, T., and Spits, H. (2011). Human IL-25- and IL-33-responsive type 2 innate lymphoid cells are defined by expression of CRTH2 and CD161. Nat. Immunol. *12*, 1055–1062.

Moretta, A., Bottino, C., Vitale, M., Pende, D., Cantoni, C., Mingari, M.C., Biassoni, R., and Moretta, L. (2001). Activating receptors and coreceptors involved in human natural killer cell-mediated cytolysis. Annu. Rev. Immunol. *19*, 197–223.

Ouyang, W., Rutz, S., Crellin, N.K., Valdez, P.A., and Hymowitz, S.G. (2011). Regulation and functions of the IL-10 family of cytokines in inflammation and disease. Annu. Rev. Immunol. *29*, 71–109.

Ryon, J.J. (2001). Isolation of mononuclear cells from tonsillar tissue. Current protocols in immunology / edited by John E. Coligan … [et al.] *Chapter 7*, Unit 7 8.

Sanos, S.L., Bui, V.L., Mortha, A., Oberle, K., Heners, C., Johner, C., and Diefenbach, A. (2009). RORgammat and commensal microflora are required for the differentiation of mucosal interleukin 22-producing NKp46+ cells. Nat. Immunol. *10*, 83–91.

Satoh-Takayama, N., Vosshenrich, C.A., Lesjean-Pottier, S., Sawa, S., Lochner, M., Rattis, F., Mention, J.J., Thiam, K., Cerf-Bensussan, N., Mandelboim, O., et al. (2008). Microbial flora drives interleukin 22 production in intestinal NKp46+ cells that provide innate mucosal immune defense. Immunity *29*, 958–970.

Satoh-Takayama, N., Dumoutier, L., Lesjean-Pottier, S., Ribeiro, V.S., Mandelboim, O., Renauld, J.C., Vosshenrich, C.A., and Di Santo, J.P. (2009). The natural cytotoxicity receptor NKp46 is dispensable for IL-22-mediated innate intestinal immune defense against Citrobacter rodentium. J. Immunol. *183*, 6579–6587.

Spits, H., and Cupedo, T. (2012). Innate lymphoid cells: emerging insights in development, lineage relationships, and function. Annu. Rev. Immunol. *30*, 647–675.

Takatori, H., Kanno, Y., Watford, W.T., Tato, C.M., Weiss, G., Ivanov, I.I., Littman, D.R., and O'Shea, J.J. (2009). Lymphoid tissue inducer-like cells are an innate source of IL-17 and IL-22. J. Exp. Med. *206*, 35–41.

Takayama, T., Kamada, N., Chinen, H., Okamoto, S., Kitazume, M.T., Chang, J., Matuzaki, Y., Suzuki, S., Sugita, A., Koganei, K., et al. (2010). Imbalance of NKp44(+)NKp46(-) and NKp44(-)NKp46(+) natural killer cells in the intestinal mucosa of patients with Crohn's disease. Gastroenterology *139*, 882–892, e881–883.

Vonarbourg, C., Mortha, A., Bui, V.L., Hernandez, P.P., Kiss, E.A., Hoyler, T., Flach, M., Bengsch, B., Thimme, R., Hölscher, C., et al. (2010). Regulated expression of nuclear receptor RORγt confers distinct functional fates to NK cell receptor-expressing RORγt(+) innate lymphocytes. Immunity *33*, 736–751.

Zenewicz, L.A., Yancopoulos, G.D., Valenzuela, D.M., Murphy, A.J., Stevens, S., and Flavell, R.A. (2008). Innate and adaptive interleukin-22 protects mice from inflammatory bowel disease. Immunity *29*, 947–957.